Magnetic Field-Induced T Cell Receptor Clustering by Nanoparticles Enhances T Cell Activation and Stimulates Antitumor Activity

Karlo Perica,[†,‡] Ang Tu,[†,‡] Anne Richter,[#] Joan Glick Bieler,[‡,⊥] Michael Edidin,[§] and Jonathan P. Schneck[†,‡,⊥,∥,*]

[†]Department of Biomedical Engineering, [‡]Institute of Cell Engineering, [§]Department of Biology, [⊥]Department of Pathology, and [∥]Departments of Oncology and Medicine, Johns Hopkins School of Medicine, Baltimore, Maryland, United States, and [#]Miltenyi Biotec, Bergisch Gladbach, Germany. K.P. and J.P.S. conceived of magnet-enhanced clustering with nano-aAPC. K.P., J.P.S., and A.R. developed approaches for generation of nano-aAPC. K.P., M.E., and J.P.S. designed experiments and wrote the manuscript. K.P., J.G.B., and A.T. performed experiments.

ABSTRACT Iron–dextran nanoparticles functionalized with T cell activating proteins have been used to study T cell receptor (TCR) signaling. However, nanoparticle triggering of membrane receptors is poorly understood and may be sensitive to physiologically regulated changes in TCR clustering that occur after T cell activation. Nano-aAPC bound 2-fold more TCR on activated T cells, which have clustered TCR, than on naive T cells, resulting in a lower threshold for activation. To enhance T cell activation, a magnetic field was used to drive aggregation of paramagnetic nano-aAPC, resulting in a doubling of TCR cluster size and increased T cell expansion *in vitro* and after adoptive transfer *in vivo*. T cells activated by nano-aAPC in a magnetic field inhibited growth of B16 melanoma, showing that this novel approach, using magnetic field-enhanced nano-aAPC stimulation, can generate large numbers of activated antigen-specific T cells and has clinically relevant applications for adoptive immunotherapy.

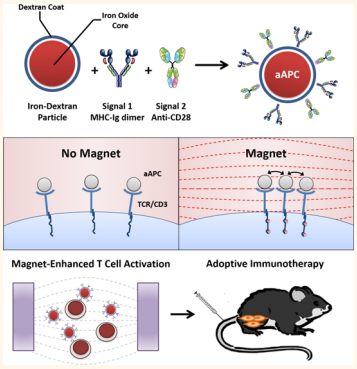

KEYWORDS: magnetic nanoparticles · cancer immunotherapy · T cell · adoptive immunotherapy · receptor clustering · membrane organization

Nanoparticles functionalized with surface ligands are frequently used for targeted delivery of drugs, proteins, and genes to cells bearing specific receptors.[1,2] Since receptor binding can trigger downstream signaling in the target cell, nanoparticle engagement of membrane receptors can also be used to directly induce biological responses.

We have previously described nanoscale artificial antigen presenting cells (nano-aAPC), 50–100 nm in diameter, as the first nanoparticles that induce antigen-specific T cell activation by presenting critical T cell activating proteins, including peptide in the context of major histocompatibility complex (MHC), to cognate T cell receptors (TCR).[3] Fixing MHC-peptide to a solid support significantly enhances T cell activation compared to soluble MHC,[3−6] which has led to the development of aAPC as vaccine platforms.

While TCR–MHC interactions have been extensively studied for MHC presented on cells[7] and cell-sized, MHC-coated particles,[8−11] receptor–ligand interactions at the cell–nanoparticle interface are not well understood and are likely to have unique properties.[12] For example, T cell activation induces a state of persistently enhanced nanoscale TCR clustering,[13−16] and nanoparticles might be sensitive to clustering at this scale in a way that larger particles are not.

Furthermore, nanoparticle interactions with TCR clusters could be exploited to enhance receptor triggering. T cell activation is mediated by aggregation of signaling proteins,[17] with "signaling clusters", 100's of nanometers across, initially forming at the periphery of the T cell–APC contact site and migrating inward.[18] We hypothesized that an external magnetic field could drive aggregation of paramagnetic nano-aAPC bound to TCR, resulting in aggregation of TCR clusters and enhanced activation of naive T cells.

Magnetic fields can exert appropriately strong forces on paramagnetic particles, but

* Address correspondence to jschnec1@jhmi.edu.

Received for review October 22, 2013 and accepted February 5, 2014.

Published online February 24, 2014
10.1021/nn405520d

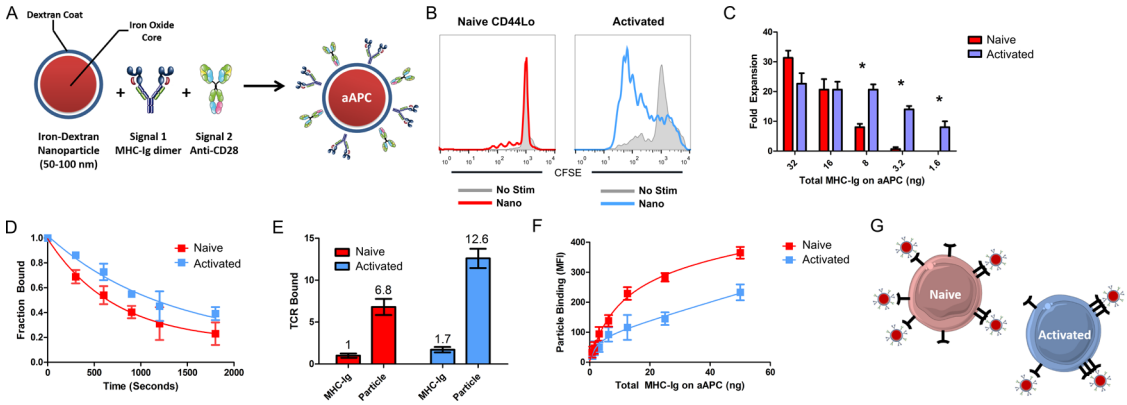

Figure 1. Nano-aAPC binding to naive and activated cells. (A) Schematic of nano-aAPC synthesis by coupling MHC-Ig dimers and co-stimulatory anti-CD28 to iron−dextran nanoparticles. (B) Proliferation of naive (left) and activated (right) pmel T cells measured by CFSE dilution 3 days after stimulation with nano-aAPC presenting 8 ng of Db-GP100. Unstimulated controls in gray. (C) Fold expansion of naive (red) and activated (blue) cells seven days after nano-aAPC stimulation. Nano-aAPC presenting 8 ng or less of MHC-Ig induced minimal proliferation in naive cells (*, $p < 0.01$) compared to activated T cells. (D) Disassociation of Kb-SIY nanoparticles bound to 2C T cells (half-lives significantly different, $p < 0.02$ by paired Student's t test; Supplementary Table 1). (E) Mean TCR−MHC contacts made between Kb-SIY dimers (MHC-Ig) and Kb-SIY nanoparticles (Particle) with naive (red) and activated (blue) cells as estimated from disassociation data ($p < 0.05$ by ANOVA with Tukey's post-test; see Supplementary Table 1). (F) Equilibrium binding of increasing doses of nano-aAPC (measured by total MHC-Ig presented) to naive (red) and activated (blue) cells ($p < 0.0001$ by two-way ANOVA). (G) Binding model that explains increased equilibrium binding and particle off-rate: naive cells bind more beads with fewer contacts per bead than activated cells.

are otherwise biologically inert, making them a powerful tool to control particle behavior.[19,20] In our approach, T cells bound to paramagnetic nano-aAPC are activated in the presence of an externally applied magnetic field. Nano-aAPC are themselves magnetized and attracted to both the field source and nearby nanoparticles in the field,[20,21] inducing bead and thus TCR aggregation to boost aAPC-mediated activation.

Here, we show that nano-aAPC bound more TCR on and induced greater activation of previously activated compared to naive T cells, consistent with the hypothesis that nano-aAPC can bind to nanoclusters of TCR. In addition, application of an external magnetic field induced nano-aAPC aggregation on naive cells, enhancing T cell proliferation *in vitro* and following adoptive transfer *in vivo*. Importantly, in a melanoma adoptive immunotherapy model, T cells activated by nano-aAPC in a magnetic field mediated tumor rejection.

RESULTS AND DISCUSSION

Nano-aAPC Preferentially Stimulate Activated T Cells. T cell stimulation requires two activating signals delivered by endogenous APC: signal 1, a cognate antigenic peptide presented in the context of MHC that binds the TCR; and signal 2, one of a number of co-stimulatory receptors that modulate T cell responses.[22] Nano-aAPC are synthesized by coupling chimeric MHC-Ig dimer (signal 1) and anti-CD28 antibody (signal 2) to 50−100 nm paramagnetic iron−dextran nanoparticles (Figure 1A), which were selected as a nanoscale particle platform due to their extensive characterization and biocompatibility.[23] Protein coupling to particles was characterized by labeling with a fluorescent antibody against the protein of interest (Supplementary Figure 1). Nano-aAPC present 13 ± 3 MHC-Ig dimers and 12 ± 5 anti-CD28 antibodies per particle, for a protein density of 96 ± 10 and 92 ± 12 protein/μm^2, respectively (Supplementary Table 1).

To compare stimulation of naive *versus* previously activated T cells, we used CD44-depleted naive CD8+ splenocytes isolated from either pmel TCR or 2C TCR transgenic mice (Supplementary Figure 2A). This technique allowed us to isolate the truly naive T cells with defined antigenic specificities, whereas our previous work[3] and the work of others[24,25] relied on mixed populations of CD44 negative and CD44 high, naive and memory cells found in transgenic mice. Activated cells were generated by stimulating CD8+ splenocytes for seven days with soluble peptide, GP100 for pmel T cells and SIY for 2C T cells.

Three days after stimulation with a low dose of nano-aAPC presenting 8 ng of total MHC-Ig, naive pmel T cells had not proliferated as measured by CFSE (Figure 1B, left), a vital dye that is diluted with each cell division. At the same dose, however, activated cells proliferated robustly (Figure 1B, right). Nano-aAPC titration showed that naive cells had a higher threshold for nano-aAPC-induced proliferation (8−10 ng of total MHC-Ig) than activated cells (less than 1.5 ng of total MHC-Ig) (Figure 1C).

As control for aAPC size, we assessed T cell proliferation induced by cell-sized, 4.5 μm diameter iron−dextran micro-aAPC. Micro-aAPC induced naive T cell proliferation at lower doses (1.5−8 ng MHC-Ig) than nano-aAPC as measured by CFSE dilution on day 3 (Supplementary Figure 2B), with approximately 10−20-fold expansion on day 7 (Supplementary Figure 2C).

Thus, while activated cells respond equivalently to nano- and micro-aAPC, naive cells have a higher threshold for nano-aAPC-based stimulation. This difference was not driven by differences in protein density between micro- and nano-aAPC, as micro-aAPC with higher density (HD) and lower density (LD) than nanoparticle-based aAPC induced identical proliferation when normalized for total MHC-Ig (Supplementary Figure 2D,E). Since response was sensitive to particle size, we hypothesized that the difference in responses was due to differences in nanoparticle interactions with TCR nanoclusters on naive *versus* activated cells.

Nano-aAPC Bind More TCR on Activated Than Naive Cells. To examine nanoparticle binding to TCR, we synthesized nanoparticles bearing MHC-Ig alone, thus removing the binding contribution of anti-CD28. Binding experiments were performed on naive and activated T cells, which bound nanoparticles bearing cognate MHC-Ig specifically and with low background (Supplementary Figure 3A).

Nanoparticles were bound to naive and activated cells to equilibrium, followed by the addition of the anticlonotypic 1B2 blocking antibody to prevent rebinding. Nanoparticles showed faster disassociation from naive cells (half-life of 531 $\pm$ 149 s) than activated cells (984 $\pm$ 221 s) ($p < 0.02$ by paired Student's *t* test) (Figure 1D, Supplementary Table 2).

Disassociation rates can be used to estimate the number of contacts between cells and multivalent ligands, with more contacts leading to slower disassociation.[26] Nanoparticle disassociation from cells was modeled as an exponential stochastic process, with disassociation of soluble MHC-Ig dimer used to derive parameters and validate the approach (see Supplementary Table 2 for details). The off-rate of a single TCR–MHC contact was measured for soluble MHC-Ig dimer binding to naive cells (Supplementary Figure 3C), which is effectively monovalent.[13] As expected, MHC-Ig dimers disassociated more slowly from activated cells, leading to 1.7 estimated contacts (Figure 1E), consistent with previous reports.[13,26]

Nanoparticle disassociation from naive cells was significantly slower than free MHC-Ig (Supplementary Figure 3C) and 2-fold slower from activated cells than naive. Nano-aAPC thus made an estimated 6.8 contacts with naive cells, compared to approximately double (12.6) on activated cells (Figure 1E, Supplementary Table 2). These numbers represent 11% and 22% of MHC-Ig dimers, respectively, attached to the surface of nano-aAPC.

Increased TCR–MHC contacts per particle could lead to fewer available TCR, inhibiting binding and limiting the total amount of nanoparticles that bind to an individual cluster. Consistent with this prediction, activated cells bound 2-fold fewer nanoparticles at equilibrium than naive cells across a wide range of particle concentrations (Figure 1F). This difference was not due to T cell receptor expression, which was equivalent on naive and activated T cells (Supplementary Figure 3B).

Together, the 2-fold increase in total nano-aAPC bound and 2-fold decrease of the TCR–MHC contacts engaged by naive cells suggest the binding model shown schematically in Figure 1G. Naive cells bind more nano-aAPC utilizing fewer MHC contacts due to the small scale of TCR clusters prior to cell–nanoparticle contact. Activated cells, in contrast, bind fewer nanoparticles because each particle makes contact with more TCR.

Magnetic Fields Drive Aggregation of aAPC and TCR/CD3. Based on the hypothesis that nano-aAPC bind to nanoscale TCR clusters, we took advantage of nanoparticle binding to control TCR cluster aggregation and, thus, T cell activation. An exogenous magnetic field was used to drive aggregation of paramagnetic nano-aAPC bound to naive cells. Nano-aAPC were bound to naive T cells at 4 °C, then cultured at 37 °C between two neodymium disk magnets generating a maximum field strength of 0.2 T. We predicted that, in an external magnetic field, paramagnetic iron–dextran aAPC would be magnetically polarized and attracted to each other,[27] driving aggregation of TCR (Figure 2A).

Cluster formation was assessed by confocal microscopy. After one hour of binding at 4 °C, we either stained and fixed cells immediately (Time 0) or transferred cells to a 37 °C incubator for 30 min in the absence or presence of a magnetic field. Cells were then stained with antibodies against LFA-1 (green), an adhesion molecule used as a control; CD3ε (magenta), a signaling component associated with TCR; and MHC-Ig (red), to visualize the nano-aAPC. Finally, cells were fixed and imaged.

Prior to incubation at 37 °C, aAPC and CD3ε were distributed in a punctate pattern on the membrane, with small clusters diffusely distributed across the cell surface (Time 0, Figure 2B, top left). LFA-1 was uniformly distributed across the cell. The LFA-1 and CD3ε staining patterns were identical to those at Time 0 after 30 min of incubation with noncognate K^b-SIINF particles (Non-Cognate, Figure 2B, top right). In the absence of a magnetic field, incubation with cognate nano-aAPC did not drastically alter the distribution of either LFA-1, aAPC, or CD3ε (No Magnet, Figure 2B, bottom left). However, after 30 min in a magnetic field, large aggregates of nano-aAPC formed on the membrane (Magnet, Figure 2B, bottom right). These clusters of nano-aAPC co-localized with similarly sized clusters of CD3ε. The control molecule LFA-1 maintained a diffuse pattern across the membrane, indicating that CD3ε aggregation was due to its association with aAPC.

To characterize the size and number of aggregates induced by aAPC, a particle-identification program was developed in ImageJ. The program was able to identify both diffuse, punctuate clusters from Time 0 cells (Figure 2C, left) and larger aggregates induced by magnetic fields (Figure 2C, right).

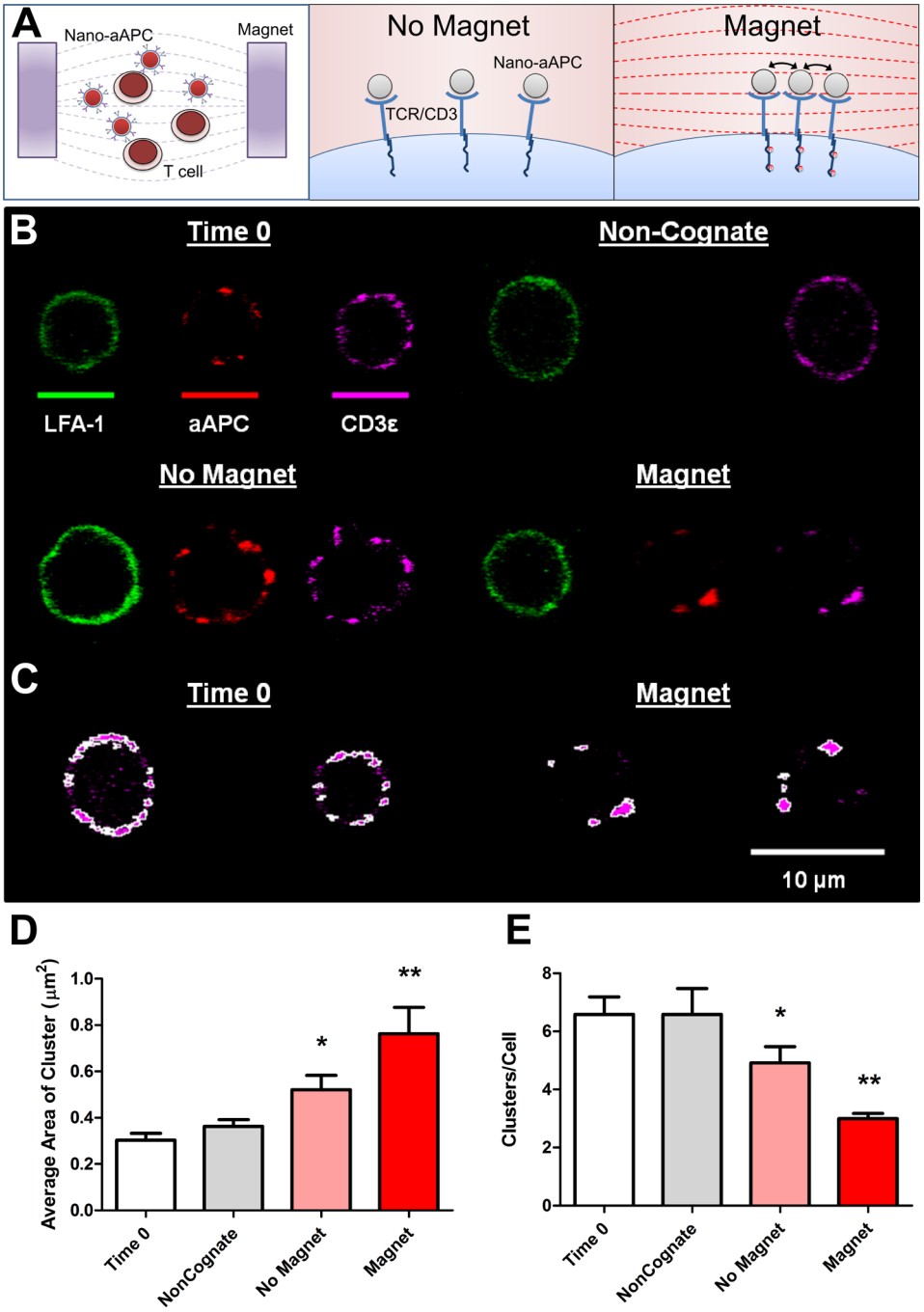

Figure 2. Clustering of aAPC and CD3ε induced by a magnetic field. (A) Schematic of magnet-induced clustering. (B) aAPC and CD3 aggregation immediately after nano-aAPC binding (Time 0) and after incubation in the presence or absence of a magnetic field. Cells were labeled with antibodies against LFA-1 (green), MHC-Ig on nano-aAPC (red), and CD3ε (magenta). Representative images are shown for cells prior to incubation (Time 0, top left), cells incubated with noncognate particles (Non-Cognate, top right), cells incubated with cognate nano-aAPC (No Magnet, bottom left), and cells incubated with cognate nano-aAPC in a magnetic field (Magnet, bottom right). (C) Aggregate detection shown for representative images from Time 0 group (two on left) and Magnet group (two on right). White outlines represent borders of CD3 clusters (magenta) identified by algorithm. (D) Average cluster area identified with cluster detection algorithm (15 cells/group). The No Magnet group had significantly larger clusters than Time 0 (*, mean difference 0.22 μm^2), and the Magnet group had significantly larger clusters than both Time 0 (, mean difference 0.46 μm^2, $p < 0.0001$ by ANOVA with Tukey post-test) and No Magnet (**, mean difference 0.24 μm^2). (E) Cells in No Magnet group had fewer clusters per cell than Time 0 (*, mean difference 5.8 clusters), and Magnet group cells had fewer clusters per cell than No Magnet (**, mean difference 1.9 clusters, $p < 0.001$ by ANOVA with Tukey post-test).**

Incubation in a magnetic field significantly increased TCR aggregation, beyond that seen after incubation with nano-aAPC alone, and led to larger CD3 complex aggregates on cells. Mean cluster area prior to incubation at 37 °C was 0.30 ± 0.03 μm^2, and this did not change after incubation with noncognate

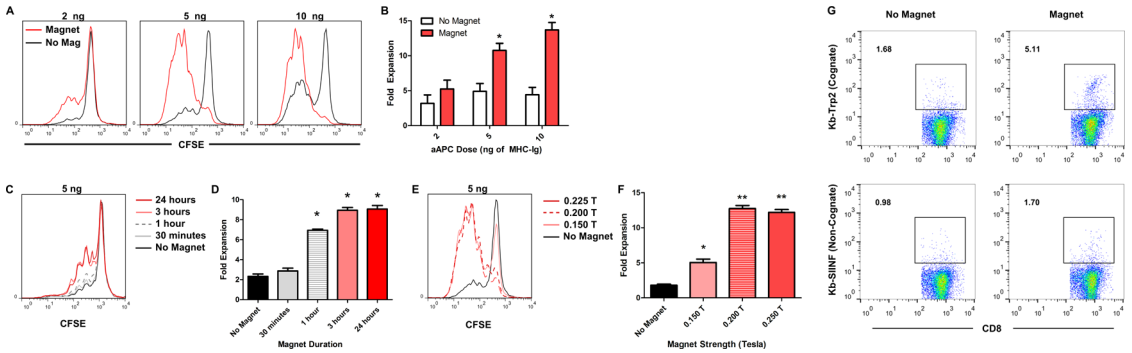

Figure 3. Magnet-enhanced nano-aAPC stimulation leads to robust T cell proliferation *in vitro*. (A) Pmel T cell proliferation by CFSE dilution three days after stimulation with nano-aAPC in the presence (red) or absence (black) of a 0.2 T external magnetic field. (B) Fold expansion of samples described in A seven days after stimulation. (C) Pmel T cells incubated with a 5 ng MHC-Ig dose of nano-aAPC and 0.2 T magnetic field for 0−24 h. Proliferation assessed by CFSE dilution at day 3. (D) Fold expansion of samples from C seven days after stimulation (*, $p < 0.001$ by ANOVA with Tukey post-test). (E) Pmel T cells incubated with a 5 ng MHC-Ig dose of nano-aAPC and magnetic fields of increasing maximal strength (0.15−0.225 T) generated by neodymium magnets of increasing thickness for 24 hours. (F) Proliferation of samples from E seven days after stimulation (* greater than no magnet, ** greater than 0.15 T magnet, $p < 0.001$ by ANOVA with Tukey post-test). (G) Antigen-specific expansion of endogenous CD8+ lymphocytes from wild-type mice after stimulation with Kb-Trp2 nano-aAPC in the presence or absence of a 0.2 T magnetic field for 24 hours. After seven days, populations were stained with cognate Kb-Trp2 (top row) or noncognate Kb-SIINF (bottom row) MHC-Ig dimer.

nano-aAPC (Figure 2D). aAPC alone increased cluster size to a mean of $0.52 \pm 0.06\ \mu m^2$ ($p < 0.001$). Clustering was further enhanced in a magnetic field to a mean size of $0.73 \pm 0.11\ \mu m^2$ ($p < 0.001$ compared to No Magnet). The mean number of clusters per cell decreased from 6.5 ± 0.6 at Time 0 to 3.0 ± 0.2 with a magnetic field (Figure 2E). Nano-aAPC disassociation rate after culture in a magnetic field did not decrease (Supplementary Figure 3D), suggesting aggregate formation was not associated with an increase in TCR/MHC contacts, but rather aggregation of TCR nanoclusters bound to aAPC.

The impact of external magnetic fields was also studied using micro-aAPC (Supplementary Figure 4A). While applying a magnetic field drove micro-aAPC aggregation, aggregation of micro-aAPC was not associated with aggregation of TCR/CD3 on cells. CD3 clusters on T cells were $0.39 \pm 0.03\ \mu m^2$ in area when incubated with micro-aAPC in the absence of a magnetic field and $0.37 \pm 0.03\ \mu m^2$ with micro-aAPC in the presence of a magnetic field (Supplementary Figure 4B,C), indicating that a magnetic field did not enhance CD3 clustering when T cells were stimulated with micro-aAPC. This is likely due to the large size of microparticles relative to TCR nanoclusters.

In summary, nano- but not micro-aAPC aggregation induced by a magnetic field led to a 2-fold increase in TCR/CD3 aggregate size and a 2-fold decrease in the number of aggregates per cell. Since receptor aggregation is known to be a strong and sufficient signal for T cell activation,[28] we examined the effect of magnet-induced TCR clustering on T cell proliferation.

Activation in a Magnetic Field Enhances Proliferation of Naive T Cells. To assess whether activation of T cells by nano-aAPC was enhanced by culture in a magnetic field, CFSE-labeled pmel T cells were incubated with increasing doses of Db-GP100 nano-aAPC and cultured with or without an external magnetic field. Naive T cells proliferated in a magnetic field at doses of nano-aAPC that induced minimal proliferation otherwise (Figure 3A). After incubation with nano-aAPC bearing 5 ng of MHC-Ig, 29% of cells in culture had proliferated, compared to 89% of cells in a magnetic field. Proliferation at day 7 was up to 4-fold greater compared to no-magnet controls (Figure 3B). Culture in a magnetic field without nano-aAPC did not lead to T cell proliferation (data not shown).

In contrast, culture with micro-aAPC in a magnetic field did not lead to enhanced T cell expansion compared to no magnet controls, as measured by both day 3 CFSE dilution and proliferation at day 7 (Supplementary Figure 4D,E).

Magnetic bead clustering has previously been used to study effects of both mechanical stress[29] and receptor clustering[21,27] in other systems, and a role has been suggested for mechanical triggering of TCR.[30,31] However, since micro-aAPC in a magnetic field are likely to transmit greater mechanical forces than nano-aAPC but do not induce TCR aggregation or enhanced proliferation, the magnet-enhanced proliferation effect seen with nano-aAPC is likely due to receptor aggregation rather than mechanical receptor "pulling".

The duration and strength of magnetic field stimulation required for optimal expansion by nano-aAPC were assessed by the addition and removal of neodymium magnets of varying size. One to three hours in a magnetic field (Figure 3C,D) and a field strength of 0.2 T or more (Figure 3E,F; Supplementary Figure 5) drove 10-fold T cell expansion after one week.

Magnetic field-enhanced aAPC stimulation also enhanced expansion of antigen-specific T cells from endogenous, polyclonal T cell populations. We synthesized nano-aAPC bearing the Kb-Ig dimer loaded with

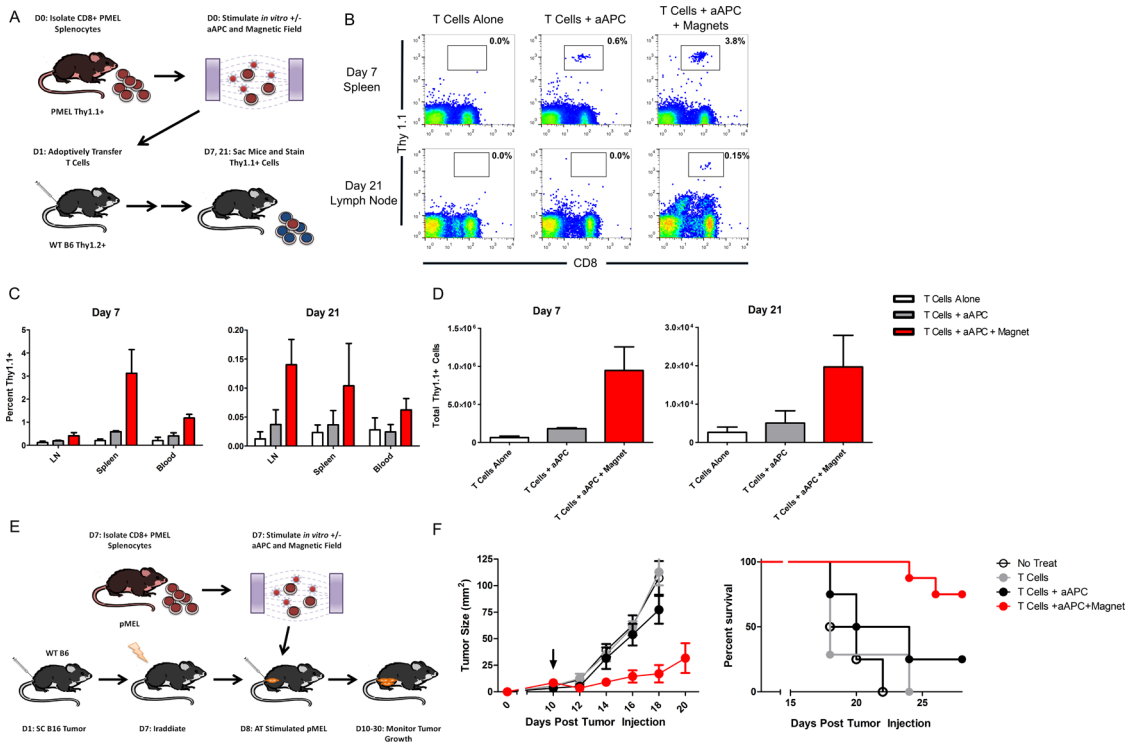

Figure 4. Magnet-enhanced T cell expansion *in vivo* and increased efficacy of adoptive immunotherapy. (A) Schematic of adoptive immunotherapy model. CD44lo, CD8+ T cells from Thy1.1+ pmel TCR transgenic mice were stimulated *in vitro* for 24 h in the presence or absence of nano-aAPC (5 ng total MHC-Ig) and magnetic field prior to being adoptively transferred into wild-type, Thy1.2+ B6 recipient mice (6 mice per group). (B) Representative frequencies of Thy1.1 cells from spleens 7 days after transfer and lymph nodes 21 days after transfer. (C) Frequencies of Thy1.1+ cells were significantly higher in mice given T cells stimulated with nano-aAPC in a magnetic field (red) compared to nano-aAPC with no magnet (gray) and no stimulation (white) ($p < 0.001$ for treatment effect by two-way ANOVA for day 7 and 21). (D) Total Thy1.1+ cells in all organs combined on day 7 and day 21. Five-fold more cells were observed in the nano-aAPC + Magnet group than nano-aAPC alone group on day 7 ($p < 0.05$ by Student's *t* test), but did not reach significance on day 21 ($p = 0.15$). (E) Schematic of treatment of established tumors with magnetic-field-enhanced adoptive immunotherapy. SC tumors were administered on day 0, partial myeloablation on day 9, and CD44lo, CD8+ pmel T cells stimulated for 24 h with either nano-aAPC (5 ng total MHC-Ig) in a magnetic field (red) or nano-aAPC with no magnet (black) were transferred on day 10. T cell alone (gray) and untreated (unfilled) groups were used as control (8 mice per group). (F) Treatment with magnet-enhanced nano-aAPC-activated T cells attenuated tumor growth compared to no magnet and control groups ($p < 0.0001$ for treatment effect by two-way ANOVA). Arrow indicates time point of adoptive transfer (day 10). Mice were censored if dead or tumors were greater than 150 mm^2. Treatment led to increased survival in T cells + nano-aAPC + Magnet group ($p < 0.001$ by Mantel−Cox log-rank test).

the Trp2 peptide, which is specific for the Trp2 melanoma antigen. CD8+ splenocytes from wild-type B6 mice were cultured with a limiting dose of aAPC, and, after seven days, antigen-specific T cells were analyzed. Nano-aAPC alone, at this dose, led to 0.70% Trp2-specific cells, as determined by comparing cognate Kb-Trp2 binding to noncognate Kb-SIINF binding (Figure 3G). When incubated with T cells in a magnetic field, however, aAPC generated approximately 3.4% antigen-specific T cells after a single week (Figure 3G). This resulted in approximately 37 000 ± 3900 Trp-2-specific cells generated from a pool of 10×10^6 precursor cells in a magnetic field, compared to 6700 ± 630 without a magnetic field (approximately 5.5-fold difference, $p < 0.01$ by Student's *t* test). With CD8 precursor frequencies estimated to be on the order of 10−800 per 10 million,[32] this suggests 450- to 3600-fold expansion in culture with a magnetic field, comparable to the 1000-fold precursor expansion seen with viral infection *in vivo*.[33]

Magnetic Field-Enhanced T Cell Activation for Adoptive Immunotherapy. The potential for enhancing stimulation of antigen-specific cells led us to study magnetic field-enhanced aAPC stimulation prior to adoptive transfer *in vivo*. Thy1.1+ pmel T cells were activated *in vitro* with aAPC in the presence or absence of a magnetic field and adoptively transferred into wild-type, Thy1.2+ recipient mice (see schematic in Figure 4A). Seven or 21 days after adoptive transfer, mice were sacrificed and assessed for adoptively transferred, Thy1.1+ cells.

Magnetic field-enhanced nano-aAPC stimulation resulted in robust expansion of the transferred T cell population. On day 7, 3.1% of T cells in the spleen were Thy1.1+ for T cells stimulated in a magnetic field, compared with 0.6% for cells stimulated with aAPC but no magnetic field, and 0.2% for untreated T cells alone that were not stimulated prior to adoptive transfer ($p < 0.01$, Figure 4B,C). The largest percentage of cells was observed in the spleen on day 7 (Figure 4C). The total Thy1.1+ cells in all organs examined reached

approximately 1×10^6 for the magnetic field-enhanced group (Figure 4D) on day 7, compared to less than 2×10^5 for the no magnet group. This 5-fold enhancement was roughly consistent with the enhancement seen *in vitro*. While fewer cells were seen on day 21, T cells activated by aAPC in a magnetic field established a detectable population in lymph nodes (0.15%), compared to 0.04% from T cells activated by aAPC alone and 0.01% from cells that were not stimulated at all ($p < 0.05$, Figure 4B–D).

The functional consequences of magnetic-field-enhanced T cell stimulation were studied by treatment of B16 melanoma, a poorly immunogenic tumor with a high threshold for immune rejection.[34] Pmel T cells were adoptively transferred into mice bearing established subcutaneous B16 tumors 10 days after tumor injection (Figure 4E), and transient lymphopenia was induced by sublethal irradiation (500 cGy) of mice one day before adoptive transfer as per standard approaches to adoptive immunotherapy.[35,36]

Tumor-specific T cells activated by aAPC in a magnetic field strongly inhibited tumor growth compared to no treatment controls, T cells alone, and T cells stimulated by aAPC without a magnetic field ($p < 0.0001$ treatment effect by two-way ANOVA, Figure 4F). At day 18, mice treated with magnetic field-enhanced T cells had 8- to 10-fold smaller tumors than untreated or no magnet T cell treated mice. Similarly, magnetic field-enhanced T cells significantly improved host survival, with 6/8 mice surviving and 4/8 having no detectable tumor at day 28 postinjection ($p < 0.001$, Mantel–Cox, Figure 4F).

CONCLUSION

Receptor triggering by nanoparticles depends on poorly understood interactions at the membrane–nanoparticle interface.[12] We demonstrate for the first time that nanoparticle binding and cellular activation are sensitive to membrane spatial organization, which is particularly important during T cell activation. We further show that magnetic fields can be used to manipulate cluster-bound nanoparticles to enhance activation.

Nanoparticle platforms are well-suited to *in vivo* administration and cellular therapy, as they are less likely than microparticles to induce tissue infarction or inflammation when co-infused with cells.[37] Iron–dextran nanoparticles are available in GMP-grade formulations, and cell isolation using magnetic enrichment followed by infusion is a staple of cellular therapy,[38,39] suggesting that magnet-induced receptor aggregation could be incorporated into immunotherapy protocols. Furthermore, magnetic fields have been used to direct trafficking of paramagnetic particles and particle-labeled cells *in vivo*,[40–42] a technique that could be coupled with magnetic clustering to direct site-specific T cell activation.

Finally, the use of applied magnetic fields allowed us to activate naive T cell populations, which were otherwise poorly responsive to stimulation. This is an important feature of immunotherapy, as naive T cells have been shown to be more effective than more differentiated subtypes for cancer immunotherapy,[43–45] with higher proliferative capacity and greater ability to generate strong, long-term T cell responses. Thus, these studies reveal a novel approach whereby nano-aAPC can potentially be coupled to magnetic field-enhanced activation of T cells to increase the yield and activity of antigen-specific T cells expanded from naive precursors, improving cellular therapy for cancer.

METHODS

Mice and Reagents. 2C TCR transgenic mice were maintained as heterozygotes by breeding on a C57/BL6 background. Pmel TCR/Thy1^a Rag−/− transgenic mice were a gift from Nicholas Restifo (National Institutes of Health, Bethesda, MD, USA) and maintained as homozygotes. C57BL/6j mice were purchased from Jackson Laboratories (Bar Harbor, ME, USA). All mice were maintained according to Johns Hopkins University's Institutional Review Board. Fluorescently labeled monoclonal antibodies were purchased from BioLegend (San Diego, CA, USA).

Preparation of MHC-Ig Dimers and Nano-aAPC. Soluble MHC-Ig dimers, K^b-Ig and D^b-Ig, were prepared and loaded with peptides as described;[8] see Supporting Information. Nano-aAPC were manufactured by direct conjugation of MHC-Ig dimer and anti-CD28 antibody (37.51; BioLegend) to MACS Microbeads (Miltenyi Biotec) as described.[3] Protein bound to nanoparticles was measured by fluorescence as described in the Supporting Information.

***In Vitro* Cell Expansion.** Cells were obtained from homogenized mouse spleens and lymph nodes followed by hypotonic lysis of red blood cells. Cytotoxic lymphocytes were isolated using a CD8 no-touch isolation kit and magnetic enrichment column from Miltenyi Biotec (Cologne, Germany). CD44-biotin antibody was added to primary cocktail to isolate CD44lo, naive cells. Where applicable, cells were labeled with carboxyfluorescein succinimidyl ester (CFSE) for 15 min at 37 °C, then washed extensively.

CD8+ T cells and nano-aAPC, at the indicated dosages, were mixed and cultured in 24-well flat-bottom or 96-well round-bottom plates for 4–7 days in complete RPMI media supplemented with T cell factor, a cytokine enriched cocktail of conditioned media harvested from stimulated human PBMC.[46] Where indicated, culture plates were fixed between two neodynium N52 disk magnets between 1/4 and 3/4 in. in length (K&J Magnetics, Jamison, PA, USA). CFSE fluorescence was measured at indicated time points using a BD FacsCalibur flow cytometer and analyzed in FlowJo (TreeStar). Fold expansion was assessed by cell counts seven days after stimulation. Expansion of endogenous antigen-specific cells was assessed by staining with 400 nM fluorescently labeled MHC-Ig dimer seven days after activation.

Particle Binding Assays. For equilibrium particle binding assays, $CD8^+$ T cells were incubated at 4 °C at a concentration of 10^7 cells/mL in FACS wash buffer (PBS + 2% FCS + 0.05% sodium azide). Aliquots (30 μL) of cells were mixed with varying concentrations of nanoparticles bearing fluorescently labeled MHC-Ig dimer for 60–90 min. After washing, cell-bound fluorescence was measured by flow cytometer, and MCF (mean channel fluorescence) was calculated using FlowJo.

For particle off-rate binding assays, cells and a saturating dose of nanoparticle or soluble MHC-Ig dimer were bound to steady state as described above. MCF was measured at time 0,

followed by the addition of excess clonotypic 1B2 blocking antibody to prevent rebinding. MCF was measured at the indicated time points, and effective off-rate was calculated for exponential decay in GraphPad Prism (La Jolla, CA, USA). Cell−particle contacts were estimated as described in Supplementary Table 2.

Microscopy. T cells were bound to nano-aAPC for 60 min at 4 °C. Cells were subsequently transferred to a 96-well plate at 37 °C in the presence or absence of a magnetic field generated by neodymium N52 disk magnets. After 30 min, cells were washed and stained at 4 °C with Alexa488 anti-LFA1, monoclonal PE anti-mouse IgG1, and Alexa 647 anti-CD3ε. Samples were washed and fixed immediately with 2% paraformaldehyde. Images were acquired on a Zeiss LSM 510 META (Zeiss, Oberkochen, Germany) laser scanning confocal microscope at 100× magnification at the Johns Hopkins School of Medicine Microscopy Facility. CD3ε cluster size was determined using a particle-detection algorithm written in ImageJ (National Institutes of Health) using the built-in particle analyzer.

Effect of Nano-aAPC on *in Vivo* T Cell Expansion and Inhibition of Subcutaneous Tumor Growth. CD44lo, CD8+ cells were isolated from pmel spleen and lymph nodes using a magnetic enrichment column and activated for 24 h in the presence or absence of a magnetic field as described above. A total of 1×10^6 Thy1.1+ pmel cells were adoptively transferred into B6 Thy1.2+ wild-type hosts ($n = 6$ mice per group). Mice were treated both the day of and the day after adoptive transfer with 30 000 units intraperitoneal IL-2. Seven and 20 days after adoptive transfer, three mice per group were sacrificed and lymphocytes were isolated from peripheral blood, spleen, and inguinal, cervical, and axillary lymph nodes and then stained with anti-Thy1.1 antibody.

Tumor rejection experiments were performed as above, except 3×10^5 B16 melanoma cells were injected subcutaneously 10 days prior to T cell adoptive transfer. Transient lymphopenia was induced by sublethal irradiation (500 cGy) one day before adoptive transfer with an MSD Nordion Gammacell dual Cs137 source (Johns Hopkins Molecular Imaging Center), as irradiation-induced lymphopenia is thought to remove immunosuppressive host cells and reduce competition for lymphotrophic cytokines[35] and significantly enhances the effect of immunotherapy for melanoma in clinical trials.[36] Tumor growth was monitored at two-day intervals using digital calipers, until tumor size was ~150 mm^2, at which point animals were euthanized.

Conflict of Interest: The authors declare the following competing financial interest(s): A.R. is an employee of Miltenyi Biotec. Under a licensing agreement between NexImmune and the Johns Hopkins University, J.P.S. is entitled to a share of royalty received by the University on sales of products derived from this article. The terms of this arrangement are being managed by the Johns Hopkins University in accordance with its conflict of interest policies.

Acknowledgment. We thank M. Paulaitis and H. Q. Mao for helpful discussions and reading of the manuscript and M. Niemöller for preparation of the nano-aAPC. This work was supported by the National Institutes of Health (P01-AI072677, R01-AI44129, and R01-CA108835) and a sponsored research agreement with Miltenyi Biotec and NexImmune. Antibody and lymphocyte images were reproduced under a Creative Commons License from Servier Medical Art (http://www.servier.com/Powerpoint-image-bank). K.P. is supported in part by a Cancer Research Institute Predoctoral Fellowship.

Supporting Information Available: Five figures and two tables. Characterization of protein conjugation to nanoparticles. Additional biophysical binding studies. Micro-aAPC expansion of T cells in the presence and absence of a magnetic field. Detailed explanation of exponential binding model. Finite element model of magnetic fields generated in culture. This material is available free of charge *via* the Internet at http://pubs.acs.org.

REFERENCES AND NOTES

1. Fay, F.; Scott, C. Antibody-Targeted Nanoparticles for Cancer Therapy. *Immunotherapy* **2011**, *3*, 381–394.
2. Moon, J. J.; Huang, B.; Irvine, D. J. Engineering Nano- and Microparticles to Tune Immunity. *Adv. Mater.* **2012**, *24*, 3724–3746.
3. Perica, K.; De León Medero, A.; Durai, M.; Chiu, Y. L.; Bieler, J. G.; Sibener, L.; Niemöller, M.; Assenmacher, M.; Richter, A.; Edidin, M.; *et al*. Nanoscale Artificial Antigen Presenting Cells for T Cell Immunotherapy. *Nanomedicine* **2013**, *10*, 119–129.
4. Luxembourg, A. T.; Brunmark, A.; Kong, Y.; Jackson, M. R.; Peterson, P. A.; Sprent, J.; Cai, Z. Requirements for Stimulating Naive CD8+ T Cells via Signal 1 Alone. *J. Immunol.* **1998**, *161*, 5226–5235.
5. Rogers, J.; Mescher, M. F. Augmentation of in Vivo Cytotoxic T Lymphocyte Activity and Reduction of Tumor Growth by Large Multivalent Immunogen. *J. Immunol.* **1992**, *149*, 269–276.
6. Motta, I.; Lone, Y. C.; Kourilsky, P. In Vitro Induction of Naive Cytotoxic T Lymphocytes with Complexes of Peptide and Recombinant MHC Class I Molecules Coated onto Beads: Role of TCR/Ligand Density. *Eur. J. Immunol.* **1998**, *28*, 3685–3695.
7. Van der Merwe, P. A.; Dushek, O. Mechanisms for T Cell Receptor Triggering. *Nat. Rev. Immunol.* **2010**, *11*, 47–55.
8. Oelke, M.; Maus, M. V; Didiano, D.; June, C. H.; Mackensen, A.; Schneck, J. P. Ex Vivo Induction and Expansion of Antigen-Specific Cytotoxic T Cells by HLA-Ig-Coated Artificial Antigen-Presenting Cells. *Nat. Med.* **2003**, *9*, 619–624.
9. Ugel, S.; Zoso, A.; De Santo, C.; Li, Y.; Marigo, I.; Zanovello, P.; Scarselli, E.; Cipriani, B.; Oelke, M.; Schneck, J. P.; *et al*. In Vivo Administration of Artificial Antigen-Presenting Cells Activates Low-Avidity T Cells for Treatment of Cancer. *Cancer Res.* **2009**, *69*, 9376–9384.
10. Oelke, M.; Schneck, J. P. Overview of a HLA-Ig Based "Lego-like System" for T Cell Monitoring, Modulation and Expansion. *Immunol. Res.* **2010**, *47*, 248–256.
11. Steenblock, E.; Wrzesinski, S.; Flavell, R.; Fahmy, T. Antigen Presentation on Artificial Acellular Substrates: Modular Systems for Flexible Adaptable Immunotherapy. *Expert Opin. Biol. Ther.* **2009**, *9*, 451–464.
12. Nel, A. E.; Mädler, L.; Velegol, D.; Xia, T.; Hoek, E. M. V; Somasundaran, P.; Klaessig, F.; Castranova, V.; Thompson, M. Understanding Biophysicochemical Interactions at the Nano-Bio Interface. *Nat. Mater.* **2009**, *8*, 543–557.
13. Fahmy, T. M.; Bieler, J. G.; Edidin, M.; Schneck, J. P. Increased TCR Avidity after T Cell Activation: A Mechanism for Sensing Low-Density Antigen. *Immunity* **2001**, *14*, 135–143.
14. Kumar, R.; Ferez, M.; Swamy, M.; Arechaga, I.; Rejas, M. T.; Valpuesta, J. M.; Schamel, W. W. A.; Alarcon, B.; van Santen, H. M. Increased Sensitivity of Antigen-Experienced T Cells through the Enrichment of Oligomeric T Cell Receptor Complexes. *Immunity* **2011**, *35*, 375–387.
15. Boyle, S.; Kolin, D. L.; Bieler, J. G.; Schneck, J. P.; Wiseman, P. W.; Edidin, M. Quantum Dot Fluorescence Characterizes the Nanoscale Organization of T Cell Receptors for Antigen. *Biophys. J.* **2011**, *101*, L57–L59.
16. Perica, K.; Bieler, J. G.; Edidin, M.; Schneck, J. Modulation of MHC Binding by Lateral Association of TCR and Coreceptor. *Biophys. J.* **2012**, *103*, 1890–1898.
17. Lillemeier, B. F.; Mörtelmaier, M. a; Forstner, M. B.; Huppa, J. B.; Groves, J. T.; Davis, M. M. TCR and Lat Are Expressed on Separate Protein Islands on T Cell Membranes and Concatenate during Activation. *Nat. Immunol.* **2010**, *11*, 90–96.
18. Varma, R.; Campi, G.; Yokosuka, T.; Saito, T.; Dustin, M. L. T Cell Receptor-Proximal Signals Are Sustained in Peripheral Microclusters and Terminated in the Central Supramolecular Activation Cluster. *Immunity* **2006**, *25*, 117–127.
19. Lee, J.-H.; Kim, E. S.; Cho, M. H.; Son, M.; Yeon, S.-I.; Shin, J.-S.; Cheon, J. Artificial Control of Cell Signaling and Growth by Magnetic Nanoparticles. *Angew. Chem., Int. Ed.* **2010**, *49*, 5698–5702.
20. Mannix, R. J.; Kumar, S.; Cassiola, F.; Montoya-Zavala, M.; Feinstein, E.; Prentiss, M.; Ingber, D. E. Nanomagnetic Actuation of Receptor-Mediated Signal Transduction. *Nat. Nanotechnol.* **2008**, *3*, 36–40.
21. Cho, M. H.; Lee, E. J.; Son, M.; Lee, J.-H.; Yoo, D.; Kim, J.-W.; Park, S. W.; Shin, J.-S.; Cheon, J. A Magnetic Switch for the Control of Cell Death Signalling in in Vitro and in Vivo Systems. *Nat. Mater.* **2012**, *11*, 1038–1043.

22. Smith-Garvin, J. E.; Koretzky, G. A.; Jordan, M. S. T Cell Activation. *Annu. Rev. Immunol.* **2009**, *27*, 591–619.
23. Kunzmann, A.; Andersson, B.; Thurnherr, T.; Krug, H.; Scheynius, A.; Fadeel, B. Toxicology of Engineered Nanomaterials: Focus on Biocompatibility, Biodistribution and Biodegradation. *Biochim. Biophys. Acta* **2010**, *1810*, 361–373.
24. Turtle, C. J.; Riddell, S. R. Artificial Antigen-Presenting Cells for Use in Adoptive Immunotherapy. *Cancer J.* **2010**, *16*, 374−381.
25. Gunn, J.; Wallen, H.; Veiseh, O.; Sun, C.; Fang, C.; Cao, J.; Yee, C.; Zhang, M. A Multimodal Targeting Nanoparticle for Selectively Labeling T Cells. *Small* **2008**, *4*, 712–715.
26. Fahmy, T. M.; Bieler, J. G.; Schneck, J. P. Probing T Cell Membrane Organization Using Dimeric MHC-Ig Complexes. *J. Immunol. Methods* **2002**, *268*, 93–106.
27. Dobson, J. Remote Control of Cellular Behaviour with Magnetic Nanoparticles. *Nat. Nanotechnol.* **2008**, *3*, 139–143.
28. James, J. R.; Vale, R. D. Biophysical Mechanism of T-Cell Receptor Triggering in a Reconstituted System. *Nature* **2012**, *487*, 64–69.
29. Hughes, S.; El Haj, A. J.; Dobson, J. Magnetic Micro- and Nanoparticle Mediated Activation of Mechanosensitive Ion Channels. *Med. Eng. Phys.* **2005**, *27*, 754–762.
30. Lim, T. S.; Mortellaro, A.; Lim, C. T.; Hämmerling, G. J.; Ricciardi-Castagnoli, P. Mechanical Interactions between Dendritic Cells and T Cells Correlate with T Cell Responsiveness. *J. Immunol.* **2011**, *187*, 258–265.
31. Husson, J.; Chemin, K.; Bohineust, A.; Hivroz, C.; Henry, N. Force Generation upon T Cell Receptor Engagement. *PLoS One* **2011**, *6*, e19680.
32. Jenkins, M. K.; Moon, J. J. The Role of Naive T Cell Precursor Frequency and Recruitment in Dictating Immune Response Magnitude. *J. Immunol.* **2012**, *188*, 4135–4140.
33. Blattman, J. N.; Antia, R.; Sourdive, D. J. D.; Wang, X.; Kaech, S. M.; Murali-Krishna, K.; Altman, J. D.; Ahmed, R. Estimating the Precursor Frequency of Naive Antigen-Specific CD8 T Cells. *J. Exp. Med.* **2002**, *195*, 657–664.
34. Klebanoff, C. A.; Gattinoni, L.; Palmer, D. C.; Muranski, P.; Ji, Y.; Hinrichs, C. S.; Borman, Z. A.; Kerkar, S. P.; Scott, C. D.; Finkelstein, S. E.; *et al*. Determinants of Successful CD8+ T-Cell Adoptive Immunotherapy for Large Established Tumors in Mice. *Clin. Cancer Res.* **2011**, *17*, 5343–5352.
35. Wrzesinski, C.; Paulos, C. M.; Kaiser, A.; Muranski, P.; Palmer, D. C.; Gattinoni, L.; Yu, Z.; Rosenberg, S. A.; Restifo, N. P. Increased Intensity Lymphodepletion Enhances Tumor Treatment Efficacy of Adoptively Transferred Tumor-Specific T Cells. *J. Immunother.* **2010**, *33*, 1–7.
36. Restifo, N. P.; Dudley, M. E.; Rosenberg, S. A. Adoptive Immunotherapy for Cancer: Harnessing the T Cell Response. *Nat. Rev. Immunol.* **2012**, *12*, 269–281.
37. Naahidi, S.; Jafari, M.; Edalat, F.; Raymond, K.; Khademhosseini, A.; Chen, P. Biocompatibility of Engineered Nanoparticles for Drug Delivery. *J. Controlled Release* **2013**, *166*, 182–194.
38. Grützkau, A.; Radbruch, A. Small but Mighty: How the MACS-Technology Based on Nanosized Superparamagnetic Particles Has Helped to Analyze the Immune System within the Last 20 Years. *Cytometry A* **2010**, *77*, 643–647.
39. Dvorak, C. C.; Gilman, a L.; Horn, B.; Oon, C.-Y.; Dunn, E. A.; Baxter-Lowe, L. A.; Cowan, M. J. Positive Selection and Transplantation of Autologous Highly Purified CD133(+) Stem Cells in Resistant/Relapsed Chronic Lymphocytic Leukemia Patients Results in Rapid Hematopoietic Reconstitution without an Adequate Leukemic Cell Purging. *Bone Marrow Transplant* **2013**, *48*, 508–513.
40. Cheng, K.; Malliaras, K.; Li, T.-S.; Sun, B.; Houde, C.; Galang, G.; Smith, J.; Matsushita, N.; Marbán, E. Magnetic Enhancement of Cell Retention, Engraftment, and Functional Benefit after Intracoronary Delivery of Cardiac-Derived Stem Cells in a Rat Model of Ischemia/Reperfusion. *Cell Transplant.* **2012**, *21*, 1121–1135.
41. Kobayashi, T.; Ochi, M.; Yanada, S.; Ishikawa, M.; Adachi, N.; Deie, M.; Arihiro, K. A Novel Cell Delivery System Using Magnetically Labeled Mesenchymal Stem Cells and an External Magnetic Device for Clinical Cartilage Repair. *Arthroscopy* **2008**, *24*, 69–76.
42. Arbab, A. S.; Jordan, E. K.; Wilson, L. B.; Yocum, G. T.; Lewis, B. K.; Frank, J. A. In Vivo Trafficking and Targeted Delivery of Magnetically Labeled Stem Cells. *Hum. Gene Ther.* **2004**, *15*, 351–360.
43. Hinrichs, C. S.; Borman, Z. a; Gattinoni, L.; Yu, Z.; Burns, W. R.; Huang, J.; Klebanoff, C. a; Johnson, L. a; Kerkar, S. P.; Yang, S.; *et al*. Human Effector CD8+ T Cells Derived from Naive Rather than Memory Subsets Possess Superior Traits for Adoptive Immunotherapy. *Blood* **2011**, *117*, 808–814.
44. Hinrichs, C. S.; Borman, Z. a; Cassard, L.; Gattinoni, L.; Spolski, R.; Yu, Z.; Sanchez-Perez, L.; Muranski, P.; Kern, S. J.; Logun, C.; *et al*. Adoptively Transferred Effector Cells Derived from Naive rather than Central Memory CD8+ T Cells Mediate Superior Antitumor Immunity. *Proc. Natl. Acad. Sci. U.S.A.* **2009**, *106*, 17469–17474.
45. Klebanoff, C. A.; Gattinoni, L.; Restifo, N. P. Sorting through Subsets: Which T-Cell Populations Mediate Highly Effective Adoptive Immunotherapy? *J. Immunother.* **2012**, *35*, 651–660.
46. Durai, M.; Krueger, C.; Ye, Z.; Cheng, L.; Mackensen, A.; Oelke, M.; Schneck, J. P. In Vivo Functional Efficacy of Tumor-Specific T Cells Expanded Using HLA-Ig Based Artificial Antigen Presenting Cells (aAPC). *Cancer Immunol. Immunother.* **2009**, *58*, 209–220.